ACS APPLIED MATERIALS & INTERFACES

Letter

www.acsami.org

Lateral Flow through a Parallel Gap Driven by Surface Hydrophilicity and Liquid Edge Pinning for Creating Microlens Array

Chengbao Jiang, Xiangming Li, Hongmiao Tian, Chunhui Wang, Jinyou Shao,* Yucheng Ding, and Li Wang

Micro-/Nano-technology Research Center State Key Laboratory for Manufacturing Systems Engineering, Xi'an Jiaotong University, 28 West Xianning Road, Xi'an, Shaanxi 710049, China

Supporting Information

ABSTRACT: This letter proposes a surface-energy driven process for economically creating polymer microlens array (MLA) with well controllable curvatures. When a UV-curable prepolymer flows into a cell constructed by multiple holes on a top template and a flat substrate, since the edge pinning of the contact line, an array of curved air/prepolymer interface forms around each microhole of the template. Then a UV-radiation of the bulk prepolymer leads to a solid microlens array. The curvature of the air/prepolymer interface can be controlled by choosing materials with different interface free energy or varying the gap height mechanically.

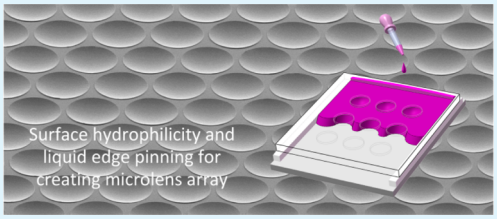

KEYWORDS: *microlens array, surface energy, hydrophilicity, liquid pinning, micromolding*

Microlens array (MLA), serving as an optical element capable of light collecting,[1] diffusing or antireflecting,[2,3] can be widely used in microelectromechanical systems,[4] optical storage devices,[5] light-emitting diodes,[6] sensors,[7] etc. Obviously, process economy, well-controlled curvature, and smooth surface would be quite desirable in the fabrication of MLA for commercial applications. So far, numerous approaches have been proposed for fabrication of MLA over a large area with a controllable curvature. They are, for example, hot embossing,[8,9] inkjet printing,[10] laser-induced polymer swelling,[11,12] thermal reflow,[13] and so on. Hot embossing, as a duplicating method, can transfer the structure of MLA from a MLA mold onto basically any thermoplastic polymer on a large area with a properly applied pressure, yet may require an expensive process for creating the MLA mold with a precise shape. Inkjet printing, a conventional approach for creating an imaging pattern of ink onto a substrate, can generate UV- or thermo-curable microdrops (or droplets) in an array digitally, without extra template or master, leading to a convex MLA after curing the droplet array for solidification. In order to obtain a spatially uniform shape for MLA, the volume of jet drops has to be consistent, requiring a precision nozzle system for the microdrop dispensing. Laser-swelling can produce MLAs on photothermally expandable polymer, in which the curvature of the MLA elements is controlled by the luminous flux of the laser beam. Thermal reflow process, based on heating of a shallow micropillar array preformed either by hot embossing or other lithography approaches, can create a MLA with a curvature defined by a properly regulated temperature. All these approaches that are well-known and other similar methods were mostly intended for fabricating a MLA with convex curvature, which would usually require an expensive or complex apparatus for adequately controlling the shape of MLA elements.

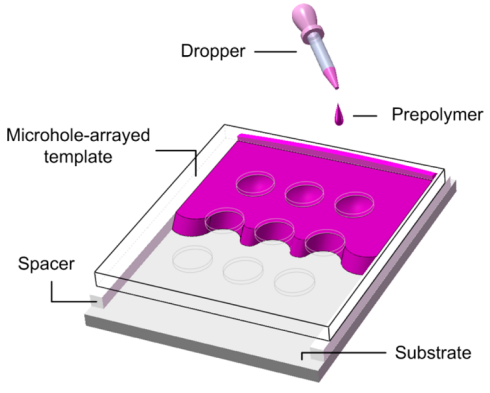

Figure 1. Illustration of the lateral flow through a parallel gap driven by surface hydrophilicity and liquid edge pinning for creating microlens array.

In practice, a MLA with concave curvature can also find unique applications, such as high-performance street lighting, biomimetic "moth-eye" surface and diffusers.[14−16] Moreover, a concave MLA with a proper mechanical and thermal strength can also serve as a master for generating a convex MLA by various micromolding processes. Comparatively, fewer researches have been reported on fabricating concave microlens. Laser ablation, wet etching and other similar material microremoving processes can produce concave MLA with

Received: September 5, 2014
Accepted: October 28, 2014
Published: October 28, 2014

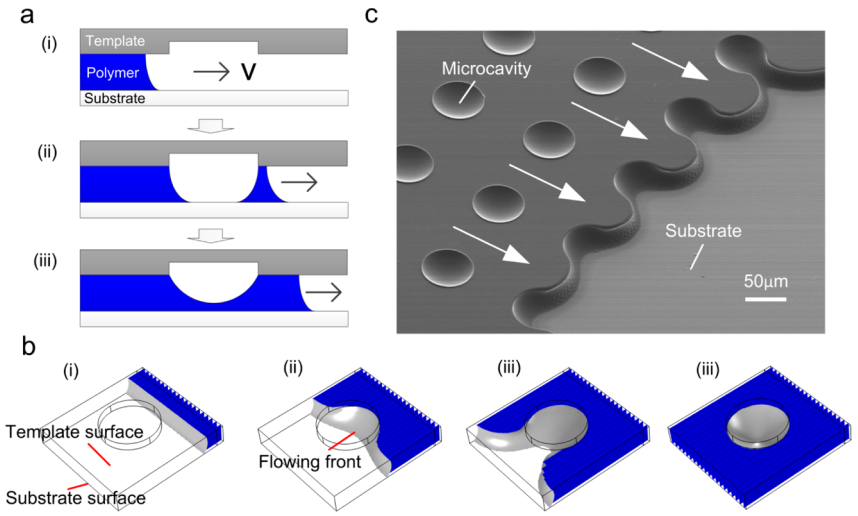

Figure 2. Hydraulic behavior of the liquid-state prepolymer flowing in a parallel air gap affected by the edge pinning of TPCL at microhole edges. (a) Illustrative formation of a bowl-shaped cavity in the prepolymer; (b) numerical simulation of the progressively moving prepolymer front; (c) SEM image of microcavities in the cured polymer after removing the template (with the arrows indicating the flow-direction of the prepolymer).

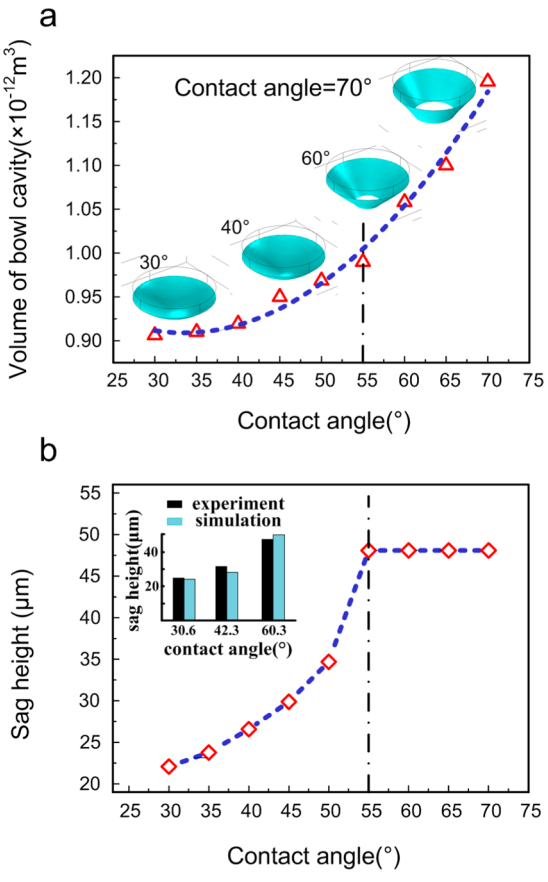

Figure 3. Dependency of the numerically obtained cavity shape on the prepolymer–substrate contact angle (at a gap height of 50 μm), showing both (a) an increasing cavity volume and (b) an increasing sag height of the cavity with the contact angle.

well-controlled shapes,[17,18] but may not be suitable for mass application because of the poor cost effectiveness or the poor surface smoothness that results from cascaded material removal. In a previous publication,[19] the authors proposed an electrowetting-based approach for generating a concave MLA with smooth surface over a large area by deforming a UV-curable prepolymer intentionally trapped inside the template microholes via an electric field. In the process, a large mechanical pressure would be required to trap the prepolymer into the air-filled template microholes. As an improvement, a process based on electrically patterned dewetting of UV curable film was presented for producing a concave MLA with a well-defined curvature,[20] using a parallel electrode pair composed of a prepolymer coated substrate and a microhole arrayed template and separated by a clearance, without a mechanical pressure. Such electrohydrodynamic processes are effective mostly only for a prepolymer with a high dielectric constant, otherwise a high voltage would be required, which may electrically cause an undesirable breakdown to the prepolymer.

In this letter, we propose a simple and economical method for creating a polymer microlens array (MLA), fully based on a surface-energy driven hydrodynamic process. The process starts with supplying an amount of a UV-curable prepolymer to one end of a parallel air gap, which is made by a hydrophilic planar plate (as the substrate) and a hydrophobically treated and microhole-arrayed template. The liquid-state prepolymer then flows laterally through this air gap throughout on the hydrophilic planar substrate due to a wettability of the prepolymer to the latter. To the contrary, on the hydrophobic template the prepolymer tends to detour around the edge of each microhole, due to an edge pinning of the progressively advancing air–liquid–solid three-phase contact line (TPCL) at the microhole opening, which prohibits the prepolymer from filling into the template along the internal vertical sidewall of the microhole. Such a prepolymer flowing will trap the air in each microhole, and more importantly, create a bowl-shaped air cavity into the prepolymer beneath each microhole opening due to the surface tension. Finally, a UV curing of the cavity arrayed prepolymer leaves on the transparent substrate a polymerized concave MLA, which is either functional optically as-is or is useable as a master for duplicating a convex MLA in a micromolding process. Our experiment and simulation presented show that the MLA curvature can be well-controlled by the substrate hydrophilicity.

A schematic for generation of a MLA with concave shape based on the surface-energy driven process is illustrated in Figure 1. A parallel air gap is made of a hydrophilic planar plate

dx.doi.org/10.1021/am506067v | ACS Appl. Mater. Interfaces 2014, 6, 18450–18456

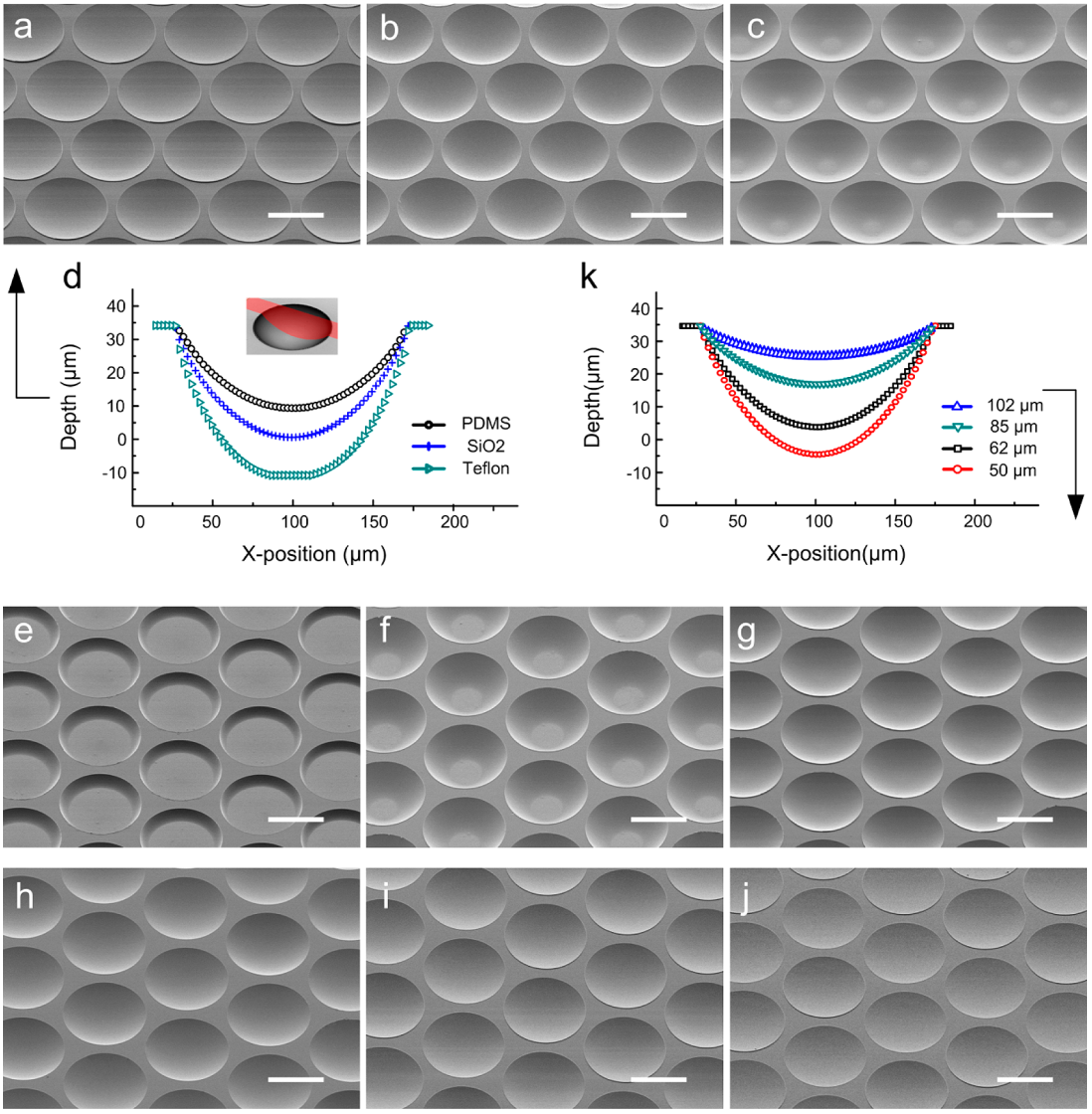

Figure 4. SEM images of MLAs fabricated at a gap height of 50 μm on (a) PDMS, (b) SiO_2, and (c) Teflon, each with (d) cross-section profile of a sampled microlens unit, and fabricated on a SiO_2 substrate at a gap height of (e) 15, (f) 30, (g) 50, (h) 62, (i) 85, and (j) 102 μm, each with (k) cross-section profile of a sampled microlens unit. The scale bar is 100 μm.

(a transparent substrate) and a planar silicon template densely arrayed with microholes and fabricated by conventional photolithography and plasma etching, with a gap height defined by the two sandwiched side spacers. A UV curable liquid-state prepolymer (NOA71, from Norland Products Inc., in our experiment) is supplied in such a sufficient amount as to block one end of the air gap. The wettability of the liquid-state prepolymer to the hydrophilic substrate drives the prepolymer to flow laterally into the gap and tends to pass spatially throughout the substrate surface. On the other hand, on the hydrophobically treated template surface (the protrusive top), the prepolymer tends to flow in a bifurcation around the opening edge of each microhole, rather than filling into the microhole along its internal vertical sidewall, due to a pinning of the moving air−liquid−solid three-phase contact line (TPCL), which occurs at the microhole's opening edge where there is a sharp change in the surface tangential, as discussed widely in other researches.[21−23]

Figure 2a shows the prepolymer flowing progressively through the parallel air gap with a cross-section of the microholes. When the moving TPCL on the template advances to the edge of a microhole, the upper prepolymer pins to the sharp edge of the microhole's opening (Figure 2a-ii), whereas the lower prepolymer on the substrate keeps progressing laterally due to the wettability and continuous tangential of the smooth substrate until passing over the microhole toward the other side of the edge to merge with the prepolymer accumulated on the template protrusion (Figure 2a-iii). Such a differential flow on the substrate and the template creates a bowl-shaped cavity under each microhole because of the surface tension. For a better understanding of the surface-energy driven process, Figure 2b shows the progressively moving prepolymer front around the edge of one single microhole based on a numerical simulation using commercial software COMSOL, which was formulated into a phase-field hydrodynamic problem with an account of surface tension and size-dependent viscosity, as described in our previous publications.[24,25] The simulation obviously shows that the prepolymer on the template (color-coded blue) is bifurcated at one side of the edge (Figure 2b-ii) and tends to merge at the other side (Figure 2b-iii). Although

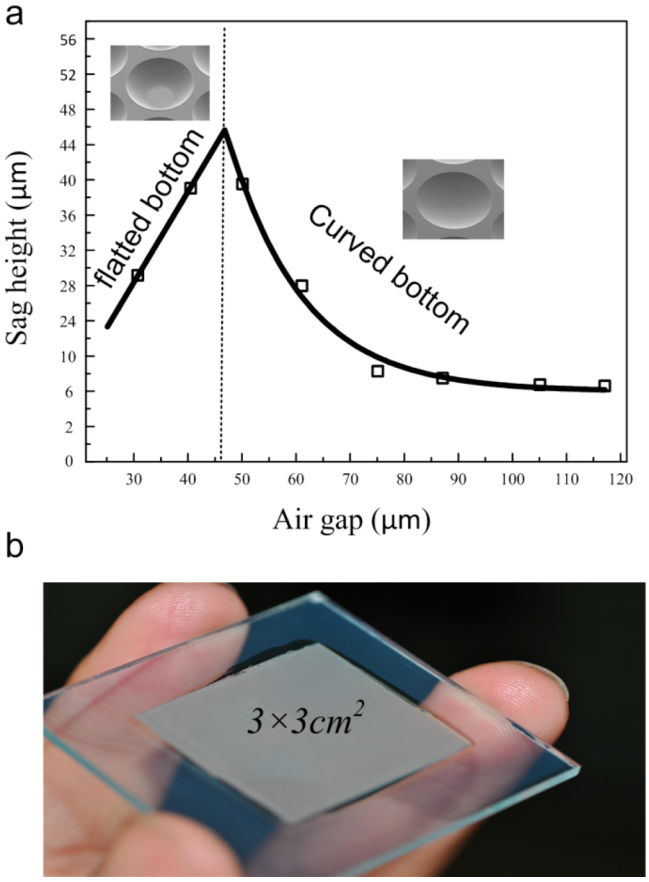

Figure 5. (a) Relationship between the sag height and the air gap; (b) photo image of a MLA fabricated on glass in an area of 3 cm × 3 cm in the curved bottom section.

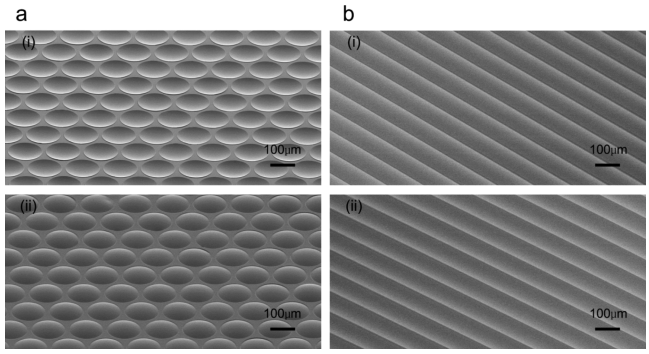

Figure 6. SEM images of convex MLAs with (a, ii) circular aperture and (b, ii) cylindrical aperture generated from (a, i and b, i) the corresponding concave MLA molds, respectively, by vacuum micromolding.

the lower prepolymer on the substrate (color-coded gray) flows overhead of the microhole to meet the prepolymer flown around the microhole later, therefore confining an air volume inside the prepolymer. This hydraulic behavior is also demonstrated by a SEM image for the UV cured polymer obtained halfway of the prepolymer flowing around microholes (Figure 2c), showing the bifurcation of the prepolymer around the microholes. In reality, the hole edges are not mathematically sharp and also have certain roughness generated during the process of dry-etching of the silicon wafer, the roughness is useful to impart additional pinning to prevent filling up of the holes when the prepolymer flow through the gap. As a liquid spreads on a structured surface the three-phase contact line often moves in a "stick and slip" manner.[26]

In our experiment, the template made from a silicon wafer was hydrophobically treated (as described in the Experimental Section) for a low surface energy, leading to a contact angle of 65° for the prepolymer on the template surface. This hydrophobic treatment on the template is preferable for a secured liquid edge pinning and an improved antiadhesion to the UV cured polymer during the template removal. The prepolymer flow in the parallel air gap can then be dominantly attributed to a capillary force produced by the wetting of the prepolymer on the substrate, as the mechanism of micromolding in capillaries (MIMIC) for generation of micro/nanostructures.[27−29] Therefore, the cavity shape in the prepolymer can be expected to be dependent on a hydrophilicity of the prepolymer to the substrate, as represented by their contact angle. Figure 3a shows an increasing volume of the bowl-shaped cavity within the prepolymer versus the prepolymer−substrate contact angle (at a gap height of 50 μm), as obtained by numerical simulation above-mentioned. The increasing cavity volume with the contact angle may be due to the fact that a large contact angle (i.e., a poor wettability) corresponds to a small driving force by the substrate, which pulls a less amount of prepolymer on the substrate beneath the confined air, leading to a small thickness of prepolymer at the bowl's bottom or a large sag height of the cavity (as shown in Figure 3b). To an extreme, when the contact angle is higher than 55°, the poorly wet substrate cannot produce a surface driving force large enough to allow the prepolymer to pass throughout the substrate overhead of the microhole, leading to a cavity shaped like a bowl with a flat bottom (as shown by the insets in Figure 3a) and to a constant sag height (being equal to the gap height) (as shown in Figure 3b). The critical contact angle should be smaller when a smaller gap height used. The viscous resistance of the prepolymer in the gap tends to increase with the decreasing gap height because of the increased shearing gradient. To avoid flat bottom cavities, the driven force, i.e., the surface-tension force, should increase correspondingly by increasing the surface energy of the substrate, i.e., decreasing its contact angle. That is, a smaller critical angle is required for a smaller gap height to avoid bottom flat cavities. The inset in Figure 3b provides a comparison of the sag height experimentally measured from the cured polymer with that numerically simulated, at three contact angles of the substrates we experimented on, justifying an accuracy of the discussion.

Figure 4a−c shows the MLAs obtained at a gap height of 50 μm by the proposed process on three transparent substrates (so that UV light can be flooded through them), i.e., PDMS, SiO_2, and Teflon, which has a measured contact angle of 32.6, 42.3, and 60.3°, respectively, to the prepolymer (NOA71) (Besides the three typical materials used to varying contact angles, which can be also effectively achieved by topographical/chemical surface treatments, such as lithography,[30] sublimation,[31] plasma techniques,[32] self-assembled monolayers,[33−35] electrochemical methods,[36] etc.). Obviously the SiO_2 substrate with a higher contact angle does lead to a higher curvature (sag height), compared to the PDMS substrate with a lower contact angle. However, the Teflon substrate with the highest contact angle tends to produce a flat-bottom bowl, undesirable as a concave microlens, meaning that a properly treated substrate is critical for generating a MLA with well-controlled shape. This observation is in agreement with the simulation presented in

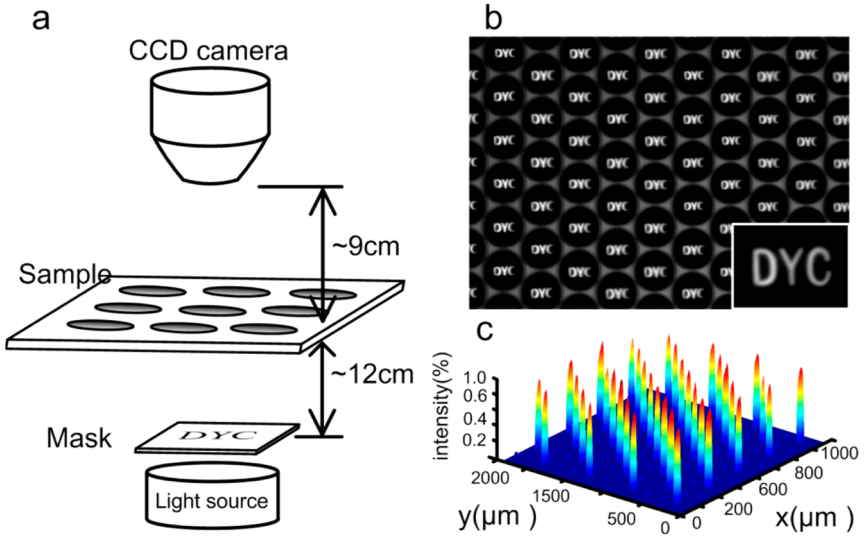

Figure 7. Demo of imaging performance of a concave MLA. (a) Illustration of experimental setup; (b) arrayed images of letter cluster "DYC" on the false focal plane of a concave MLA; (c) normalized light intensity profile of a MLA with sag height of ~35 μm.

Figure 3. Additionally, Figure 4d provides the cross-section profile for one sampled unit of each corresponding MLA, as obtained by a laser scanning confocal microscope (LSCM), which shows that the MLA obtained on the poorly wet Teflon has the same sag height as the gap height, proving that the prepolymer has not flown throughout this substrate.

It is important to note that the prepolymer's lateral flow in the parallel air gap also undergoes a viscous resistance while driven by the substrate. The velocity field of the prepolymer flow would be too complicated to map analytically for characterizing the viscous resistance due to an existence of the microholes. However, one thing for sure is that such a viscous resistance can be expected to increase with the decreasing gap height because the latter tends to produce an increased shearing gradient, considering the fact the prepolymer advances laterally on the lower substrate while pinning at the microhole edge of the upper template. This implies that for a small gap height the driving force on the substrate may not be large enough to overcome the viscous resistance in order to pass throughout the substrate overhead of the microholes, leading to a concave with smooth bottom (in which the trapped cavity air is in contact with the naked substrate). Figure 4e–j show the SEM images for the prepolymer cavity array obtained on SiO_2 at increasing gap height. The undesirable even-bottom cavities obtained at a small gap height (15 μm for Figure 4e and 30 μm for Figure 4f) indicate that the prepolymer has not flown throughout the substrate, as proved by the sag height in the LSCM acquired cross-section profiles of the cavities in which the sag heights are the same as the corresponding gap heights. Therefore, for a certain substrate, a gap height large enough would be required to allow the prepolymer to flow throughout the substrate for creating a fully trapped cavity, as shown in Figure 4g–j. However, with the further increasing of the gap height, the sag height of the fully trapped cavity tends to decline as indicated in Figure 4k. The dependency of cavity shape on the gap height can be seen clearly in Figure 5a, which can be divided into two parts as indicated by the dotted line. In the first part, the cavities have even-bottoms and the sag heights linearly increase with the air gap. In the second part, the bottoms of the cavities were curved and the corresponding sag heights decreased with the gap height. The reason is also because the decreased tangential resistance in larger air gaps leads to more amount of prepolymer through the substrate under the holes. The critical gap height between the two parts can be figured out at the interaction of the curves and is about 46 μm. The MLA can be fabricated in an area as large as 3 cm × 3 cm on glass at a gap height of 50 μm, as shown in Figure 5b.

The concave polymer (NOA71) MLA generated as described above either is optically functional as-is in some unique applications (mentioned in the beginning part of this letter), or can be used as a master for duplicating a convex MLA by a vacuum micromolding process.[37] In our experiment, the concave MLA master (of UV-cured NOA71) was coated with an antiadhesion C_4F_8 layer with a thickness of roughly 50 nm by inductively coupled plasma chemical vapor deposition (ICP-CVD) to ease the subsequent demolding. First, the liquid-state NOA71 prepolymer was properly distributed on the master. A glass slide was then pressed against the master to sandwich the prepolymer between them into a proper thickness. The micromolding was performed in a vacuum so that the NOA71 prepolymer fully fill onto the master's concave surface without air trapping. A UV flooding on the sandwiched prepolymer and removal of the master led to a convex MLA on the glass slide, as shown in Figure 6a-ii.

Obviously by using a template arrayed with parallel gratings, the proposed process can also be easily used for generating MLA with a cylindrical curvature, which may find applications such as collimating high-power diode lasers,[38] homogenizing and transforming the laser beam,[39] organic light-emitting diode (OLED) panel,[40] etc. Figure 6b shows a MLA with a concave cylindrical curvature (i) and its duplicate as a MLA with a convex cylindrical curvature obtained by micromolding (ii).

To demonstrate the focal performance of the MLA, we performed an imaging test, as shown in Figure 7a. A concave MLA was positioned vertically on a motion stage and moved relatively to a CCD camera. The MLA was illuminated with a white light from behind a mask with a pattern of letter cluster DYC, which was fabricated by laser ablation of a Cr film sputtered on a glass slide. Then, on the false focal plane of the concave MLA, an array of bright false and reduced image of the letter cluster could clearly be observed through the CCD camera, as shown in Figure 7b. When the mask was replaced by

another mask with an optical aperture, an array of sharply focused light spot was obtained, and its light intensity (represented in a normalized gray) is shown in Figure 7c.

In a final summary, the presented process for generation of a concave polymer MLA is economical and well controllable due to the fact that it simply uses the differential surface energy on a hydrophilic substrate and a hydrophobically treated and microhole-arrayed silicon template that can be fabricated easily by conventional photolithography and plasma etching. The curvature of the MLAs can be tuned by two approaches: varying the contact angle of a transparent substrate or varying the gap height. In contrast, the approach of mechanical change of the gap height is more attractive to mass-produce of MLAs since the simply using of PI-spacers or a more precisely control the gap height with mechanical tools. The process of chemical treatment to the substrate for different contact angles is usually time-consuming or high-cost because of complex equipment and expensive materials.

■ ASSOCIATED CONTENT

Supporting Information

Experimental details. This material is available free of charge via the Internet at http://pubs.acs.org.

■ AUTHOR INFORMATION

Corresponding Author

*E-mail: jyshao@mail.xjtu.edu.cn.

Notes

The authors declare no competing financial interest.

■ ACKNOWLEDGMENTS

Mr. Chengbao Jiang and Xiangming Li, the first two authors, are the graduate students of the corresponding author, and has contributed equally to this work, which is financed by the NSFC Major Research Plan on Nanomanufacturing (Grant 91323303), and NSFC Funds (Grants 51275401 and 51175417).

■ REFERENCES

(1) Tripathi, A.; Chokshi, T.; Chronis, N. A High Numerical Aperture, Polymer-Based, Planar Microlens Array. *Opt. Express* **2009**, *17*, 19908−19918.

(2) Chang, S.; Yoon, J. Microlens Array Diffuser for a Light-Emitting Diode Backlight System. *Opt. Lett.* **2006**, *31*, 3016−3018.

(3) Jung, H.; Song, C.; Jeong, K. Monolithic Polymer Microlens Arrays with Antireflective Nanostructures. *Appl. Phys. Lett.* **2012**, *101*, 203102.

(4) Gokce, S.; Holmstrom, S.; Hibert, C.; Olcer, S.; Bowman, D.; Urey, H. Two-Dimensional MEMS Stage Integrated with Microlens Arrays for Laser Beam Steering. *J. Microelectromech. Syst.* **2011**, *20*, 15−17.

(5) Kim, H.; Lee, J.; Lim, J.; Kim, S. M.; Kang, S.; Hendriks, R.; Kastelijn, A.; Busch, C.; *International Symposium on Optical Memory and Optical Data Storage*, Honolulu Hawaii, 7, 2005.

(6) Li, X.; Zhu, P.; Liu, G.; Zhang, J.; Song, R.; Ee, Y. Light Extraction Efficiency Enhancement of III-Nitride Light Emitting Diodes by Using 2-D Close-Packed TiO_2 Microsphere Arrays. *J. Dispersion Technol.* **2013**, *9*, 324−332.

(7) Nussbaum, P.; Völkel, R.; Herzig, H.; Eisner, M.; Haselbeck, S. Desigh, Fabrication and Testing of Microlens Arrays for Sensors and Microsystems. *Pure Appl. Opt.* **1997**, *6*, 617−636.

(8) Ong, N.; Koh, Y.; Fu, Y. Microlens Array Produced Using Hot Embossing Process. *Microelectron. Eng.* **2002**, *60*, 365−379.

(9) Chang, C.; Yang, S.; Huang, L.; Chang, J. Fabrication of Plastic Microlens Array Using Gas-Assisted Micro-Hot-Embossing with a Silicon Mold. *Infrared Phys. Technol.* **2006**, *48*, 163−173.

(10) Kim, J.; Brauer, N.; Fakhfouri, V.; Boiko, D.; Charbon, E.; Grutzner, G. Hybrid Polymer Microlens Arrays with High Numerical Apertures Fabricated Using Simple Ink-Jet Printing Technique. *Opt. Mater. Express* **2011**, *1*, 259−269.

(11) Shao, J.; Ding, Y.; Zhai, H.; Hu, B.; Li, X.; Tian, H. Fabrication of Large Curvature Microlens Array Using Confined Laser Swelling Method. *Opt. Lett.* **2013**, *38*, 3044−3046.

(12) Shao, J.; Ding, Y.; Wang, W.; Mei, X.; Zhai, H.; Tian, H. Generation of Fully-Covering Hierarchical Micro/nano Structures by Nanoimprinting and Modified Laser Swelling. *Small* **2014**, *10*, 2595−2601.

(13) He, M.; Yuan, X.; Ngo, N.; Bu, J.; Kudryashov, V. Simple Reflow Technique for Fabrication of a Microlens Array in Sol-Gel Glass. *Opt. Lett.* **2003**, *28*, 731−733.

(14) Lee, X.; Moreno, I.; Sun, C. High-Performance LED Street Lighting Using Microlens Arrays. *Opt. Express* **2013**, *21*, 10612−10621.

(15) Ko, D.; Tumbleston, J.; Henderson, K.; Euliss, L.; Desimone, J.; Lopez, R. Biomimetic Microlens Array with Antireflective "Moth-Eye" Surface. *Soft Matter* **2011**, *7*, 6404−6407.

(16) Ruffieux, P.; Scharf, T.; Philipoussis, I.; Herzig, H.; Voelkel, R.; Weible, K. Two-Step Process for the Fabrication of Diffraction Limited Concave Microlens Arrays. *Opt. Express* **2008**, *16*, 19541−19549.

(17) Lin, C.; Jiang, Y.; Xiao, H.; Chen, S.; Tsai, H. Fabrication of Microlens Arrays in Photosensitive Glass by Femtosecond Laser Direct Writing. *Appl. Phys. A: Mater. Sci. Process.* **2009**, *97*, 751−757.

(18) Oh, H.; Kim, G.; Seo, H.; Song, Y.; Lee, K.; Yang, S. Fabrication of Micro-Lens Array Using Quartz Wet Etching and Polymer. *Sens. Actuators, A* **2010**, *164*, 161−167.

(19) Li, X.; Ding, Y.; Shao, J.; Tian, H.; Liu, H. Fabrication of Microlens Arrays with Well-Controlled Curvature by Liquid Trapping and Electrohydrodynamic Deformation in Microholes. *Adv. Mater.* **2012**, *24*, OP165−169.

(20) Li, X.; Tian, H.; Ding, Y.; Shao, J.; Wei, Y. Electrically Template Dewetting of a UV-Curable Prepolymer Film for the Fabrication of a Concave Microlens Array with Well-Defined Curvature. *ACS Appl. Mater. Interfaces* **2013**, *5*, 9975−9982.

(21) Oliver, J.; Huh, C.; Mansion, S. Resistance to Spreading of Liquid by Sharp Edges. *J. Colloid Interface Sci.* **1977**, *59*, 568−581.

(22) Liimatainen, V.; Sariola, V.; Zhou, Q. Controlling Liquid Spreading Using Microfabricated Undercut Edges. *Adv. Mater.* **2013**, *25*, 2275−2278.

(23) Fang, G.; Amirfazli, A. Understanding the Edge Effect in Wetting: a Thermodynamic Approach. *Langmuir* **2012**, *28*, 9421−9430.

(24) Tian, H.; Shao, J.; Ding, Y.; Li, X.; Liu, H. Numerical Characterization of Electrohydrodynamic Micro- or Nanopatterning Processes Based on a Phase-Field Formulation of Liquid Dielectrophoresis. *Langmuir* **2013**, *29*, 4703−4714.

(25) Tian, H.; Shao, J.; Ding, Y.; Li, X.; Li, X. Numerical Studies of Electrically Induced Pattern Formation by Coupling Liquid Dielectrophoresis and Two-Phase Flow. *Electrophoresis* **2011**, *32*, 2245−2252.

(26) Oliver, J.; Mason, S. Microspreading Studies on Rough Surface by Scanning Electron Microscopy. *J. Colloid Interface Sci.* **1977**, *60*, 480−487.

(27) Xia, Y.; Kim, E.; Whitessides, G. Micromolding of Polymers in Capillaries: Applications in Microfabrication. *Chem. Mater.* **1996**, *8*, 1558−1567.

(28) Kim, E.; Whitesides, G. Imbibition and Flow of Wetting Liquids in Noncircular Capillaries. *J. Phys. Chem. B* **1997**, *101*, 855−863.

(29) Kim, E.; Xia, Y.; Whitesides, G. Micromolding in Capillaries: Applications in Materials Science. *J. Am. Chem. Soc.* **1996**, *118*, 5722−5731.

(30) Didem, Ö.; Thomas, J. Ultrahydrophobic Surface. Effects of Topography Length Scales on Wettability. *Langmuir* **2000**, *16*, 7777−7782.
(31) Nakajima, A.; Hashimoto, K.; Watanabe, T. Transparent Superhydrophobic Thin Films with Self-Cleaning Properties. *Langmuir* **2000**, *16*, 7044−7047.
(32) Coulson, S.; Woodward, I.; Badyal, J. Ultralow Surface Energy Plasma Polymer Films. *Chem. Mater.* **2000**, *12*, 2031−2038.
(33) Xia, F.; Jiang, L. Bio-Inspired, Smart, Multiscale Interfacial Materials. *Adv. Mater.* **2008**, *20*, 2842−2858.
(34) Elliott, G.; Riddiford, A. Dynamic contact angle: 1. The Effect of Impressed Motion. *J. Colloid Interface Sci.* **1967**, *23*, 389−398.
(35) Li, X.; Shao, J.; Tian, H.; Ding, Y.; Li, X. Fabrication of High-Aspect-Ratio Microstructures Using Dielectrophoresis-Electrocapillary Force-Driven UV-Imprinting. *J. Miromech. Microeng.* **2011**, *21*, 65010−65018.
(36) Zhang, X.; Shi, F.; Yu, X.; Liu, H.; Wang, Z.; Jiang, L.; Li, X. Polyelectrolyte Multilayer as Matrix for Electrochemical Deposition of Gold Clusters: Toward Super-Hydrophobic Surface. *J. Am. Chem. Soc.* **2004**, *126*, 3064−3065.
(37) Xia, Y.; Whitesides, G. M. Soft Lithography. *Adv. Mater.* **1998**, *37*, 550−575.
(38) Possner, T.; Messerschmidt, B.; Kraplin, A.; Blumel, V.; Hofer, B.; Schreiber, P. Assembly of Fast-Axis Collimating Lenses with High Power Laser Diode Bars. *Proc. SPIE* **2000**, *3952*, 392−399.
(39) Sinhoff, V.; Hambuecher, S.; Kleine, K.; Ruebenach, O.; Wessling, C. Miro-Lens Arrays for Laser Beam Homogenization and Transformation. *Proc. SPIE* **2013**, *8605*, 860509−860515.
(40) Lee, J.; Ho, Y.; Chen, K.; Lin, H.; Fang, J.; Hsu, S. Efficiency Improvement and Image Quality of Organic Light-Emitting Display by Attaching Cylindrical Microlens Arrays. *Opt. Express* **2008**, *16*, 21184−21190.